

1 Improving the elevated-temperature properties by two-step heat treatments
2 in Al-Mn-Mg 3004 alloys

3 K. Liu*, H. Ma and X.-Grant Chen

4
5 Department of Applied Science, University of Quebec at Chicoutimi,
6 Saguenay, QC, Canada, G7H 2B1

7 Corresponding author: kun.liu@uqac.ca; Tel.: 1-4185455011 ext.7112; Fax: 1-4185455012

8 **Abstract**

9 In the present work, two-step heat treatments with preheating at different
10 temperatures (175, 250 and 330 °C) as the first step followed by the peak precipitation
11 treatment (375°C/48h) as the second step have been performed in Al-Mn-Mg 3004 alloys
12 to study their effects on the formation of dispersoids and the evolution of the elevated-
13 temperature strength and creep resistance. During the two-step heat treatments, the
14 microhardness is gradually increasing with increasing time until to a plateau after 24
15 hours when first treated at 250 °C and 330 °C, while there is a minor decrease with time
16 when first treated at 175 °C. Results show that both the yield strength and creep
17 resistance at 300 °C reach the peak values after the two-step treatment of
18 250°C/24h+375°C/48h. The formation of dispersoids is greatly related to the type and
19 size of pre-existing Mg₂Si precipitated during the preheating treatments. It was found that
20 coarse rod-like β'-Mg₂Si strongly promotes the nucleation of dispersoids while fine
21 needle-like β''-Mg₂Si has less influence. Under optimized two-step heat treatment and
22 modified alloying elements, the yield strength at 300 °C can reach as high as 97 MPa
23 with the minimum creep rate of 2.2×10⁻⁹ s⁻¹ at 300 °C in Al-Mn-Mg 3004 alloys, enabling
24 them as one of the most promising candidates in lightweight aluminum alloys for
25 elevated-temperature applications.

26 **Key words:** Al-Mn-Mg alloy; two-step heat treatments; dispersoids; nucleation;
27 elevated-temperature properties.

28 **Introduction**

29 Due to the rapid demand from weight-sensitive automotive and aerospace industrials
30 for the lightweight materials, such as aluminum alloys on the elevated-temperature
31 applications, Al-Mn 3xxx alloys has been developed to obtain the good properties at both
32 room temperature (RT) and elevated temperature, in which the dispersoid-strengthening
33 mechanism plays a significant role [1-4]. Typical industrial applications of Al-Mn 3xxx
34 alloys can be found in the fabrication of the can body used at room temperature and the
35 heat exchanger applied at elevated temperature [5, 6]. In our previous works [2, 3, 7-9],
36 the yield strength and creep resistance at 300 °C of Al-Mn-Mg 3004 alloy were improved

37 by modifying the alloying elements, such as Mn, Fe, Mo and addition of TiB₂ nano-
38 particles, to optimize the characters of dispersoids, including the size, volume fraction
39 and distribution. For instance, Mo was introduced in 3004 alloy to increase the volume
40 fraction of dispersoids and reduce the area of the dispersoid free zone (DFZ), leading to a
41 significant increase on both the strength and creep resistance at 300 °C [7]. On the other
42 hand, the mechanical properties became worse at high Fe content due to its consumption
43 of Mn to form Al₆(MnFe) intermetallics, resulting in less available Mn solutes for the
44 precipitation of dispersoids [3]. Therefore, optimizing the characters of dispersoids is
45 always the key factor to improve the elevated-temperature properties of dispersoid-
46 strengthened aluminum alloys for elevated-temperature applications.

47 In addition to modifying the alloying elements, the heat treatment has been reported
48 to have a significant influence on the precipitation of dispersoids [1, 2, 4, 10-13]. It is
49 found that the dispersoids changed from α -Al(MnFe)Si to Al₆(MnFe) when the
50 temperature of heat treatment was higher than 600 °C in 3003 alloys [10, 12], while only
51 α -Al(MnFe)Si dispersoids were observed in 3004 alloys due to its high Si content [2]. In
52 addition, the volume fraction of dispersoids decreased with increasing homogenization
53 temperature [1, 2, 7, 11]. Conventionally, the Al-Mn 3xxx alloys are classified as non-
54 heat-treatable alloys. The only heat treatment is the homogenization before rolling or
55 extrusion, which is typically carried out at 600 °C for several hours. For newly-developed
56 Al-Mn 3xxx alloys, the heat treatment is performed at 375-450 °C to promote the
57 precipitation of a large number of dispersoids [2]. It is reported that the volume fraction
58 of dispersoids decreased from 2.95 vol.% after 375°C/48h to 1.94 vol.% after 425°C/48h,
59 resulting in the decrease of the yield strength (YS) at 300 °C from 78 MPa to 65 MPa in
60 3004 alloys [2]. Similar tendency was also reported in 3003 alloys that YS at RT
61 decreased from 87 MPa after 375°C/24h to 73 MPa after 450°C/0.5h [11].

62 However, most of the heat-treatments performed in the literatures are the single step
63 treatment with a temperature higher than the precipitation temperature of dispersoids in
64 3xxx alloys (~ 340°C [2]). On the other hand, it is suggested that the stepwise heat
65 treatment was helpful for the nucleation and distribution of Al₃Zr dispersoids in 7xxx
66 alloys [14-18], which consists of the preheating treatment at a low temperature as the first
67 step followed by the conventional precipitation treatment at a high temperature. The first
68 preheating treatment was designed to create a favorable condition of Al₃Zr dispersoid
69 nucleation. It is reported that two-step heat treatment can minimize the precipitation-free
70 zones and greatly increased the number density of dispersoids in 7150 aluminum alloy
71 [15]. However, there is no open literature available for the influence of the two-step heat
72 treatment on the evolution of dispersoids and elevated-temperature properties in Al-Mn
73 3xxx alloys.

74 In the present work, various two-step heat treatments with the preheating treatments
75 at 175, 250 and 330 °C as the first step followed by the peak precipitation treatment as
76 second step are applied on Al-Mn-Mg 3004 alloys. The formation of dispersoids during

77 two-step heat treatments is quantitatively analyzed to establish the relationship between
78 the two-step heat treatment, dispersoid precipitation and the elevated-temperature
79 strength and creep resistance. In addition, the potential of further improvement of
80 elevated-temperature properties under optimized two-step heat treatment and modified
81 chemical composition are demonstrated for Al-Mn 3xxx alloys.

82 2. Experimental

83 Two experimental Al-Mn-Mg 3004 alloys were prepared using commercially pure
84 Al (99.7%), pure Mg (99.9%), Al-25%Mn, Al-25%Fe and Al-50%Si master alloys. Alloy
85 A is the base alloy with traditional alloying elements while Alloy B is the alloy with
86 modified chemical composition by adjusting Mn, Fe and Mo alloying elements, designed
87 for enhancing elevated-temperature properties according to the literature [3, 7, 8]. In each
88 batch, approximately 3 kg of material was prepared in a clay-graphite crucible using an
89 electric resistance furnace. The temperature of the melt was maintained at ~750°C for 30
90 min. The melt was degassed for 15 min and then poured into a permanent mold preheated
91 at 250°C. The dimension of the cast ingots was 30mm×40mm×80mm. The chemical
92 compositions of the experimental 3004 alloys analyzed using an optical emission
93 spectrometer are shown in Table 1 (all of the alloy compositions are in wt. % unless
94 indicated otherwise).

95 During the two-step heat treatment, the Alloy A was first heat-treated at 175, 250
96 and 330 °C for up to 48 hours as the first step followed by water quench, and then heated
97 to 375 °C for 48h as the second step followed by the water quench at RT. The heating
98 rate for all treatments is controlled at 250 °C/h. As a reference, the single-step heat
99 treatment (375°C/48h) was also performed to compare with the properties after two-step
100 heat treatments. In addition, the best two-step heat treatment was selected and applied on
101 Alloy B to explore the further improvement of elevated-temperature properties.

102 After heat treatments, the samples were polished for metallographic observations
103 and machined for mechanical and creep tests. To reveal the dispersoids clearly, the
104 polished samples were etched in 0.5% HF for 30 seconds. An optical microscopy (OM)
105 and a scanning electron microscopy (SEM) were used to observe the as-cast and heat-
106 treated microstructures. A transmission electron microscope (TEM) was used to observe
107 the distribution of dispersoids in the dispersoid zone. The thickness of the TEM sample
108 was measured with an electron energy loss spectroscopy (EELS) equipped on TEM. The
109 size and number density of dispersoids were measured using the image analysis on TEM
110 images. In this study, the volume fraction of DFZ was converted from the area fraction of
111 DFZ measured in the image analysis from optical images according to Delesse's principle
112 [19, 20], while the volume fraction of dispersoids was calculated according to the method
113 introduced in the literature [4] and is shown in Eq. (1):

$$114 \quad V_v = A_d \frac{\overline{KD}}{\overline{KD} + t} (1 - A_{DFZ}) \quad (1)$$

115 where \bar{D} is the average equivalent diameter of dispersoids; t is the TEM foil
116 thickness; A_d is the area percentage of dispersoids from TEM observation; A_{DFZ} is the
117 area percentage of DFZ from OM measurements; and \bar{K} is the average shape factor of
118 dispersoids.

119 Additionally, Vickers microhardness, YS and creep properties were measured after
120 various heat treatments. Among these properties, microhardness is measured at RT while
121 mechanical property (YS) and creep resistance were tested at 300 °C. The YS at 300 °C
122 was obtained from compression tests at a strain rate of 10^{-3} 1/s, which were performed on
123 a Gleeble 3800 thermomechanical simulator unit using cylindrical specimens (15 mm in
124 length and 10 mm in diameter). For the compression test at 300 °C, the specimen was
125 heated to the required temperatures with a heating rate of 2 °C/s and held for 3 minutes to
126 stabilize. An average value of YS was obtained from 3 tests. The compressive creep tests
127 were performed at 300 °C for 100 hours with a constant load of 45 MPa. The creep
128 specimens were the same size as the Gleeble samples and 3 tests were repeated to
129 confirm the reliability of the results at each condition. Details of test methods can be
130 found in the reference [2].

131 **3. Results and discussion**

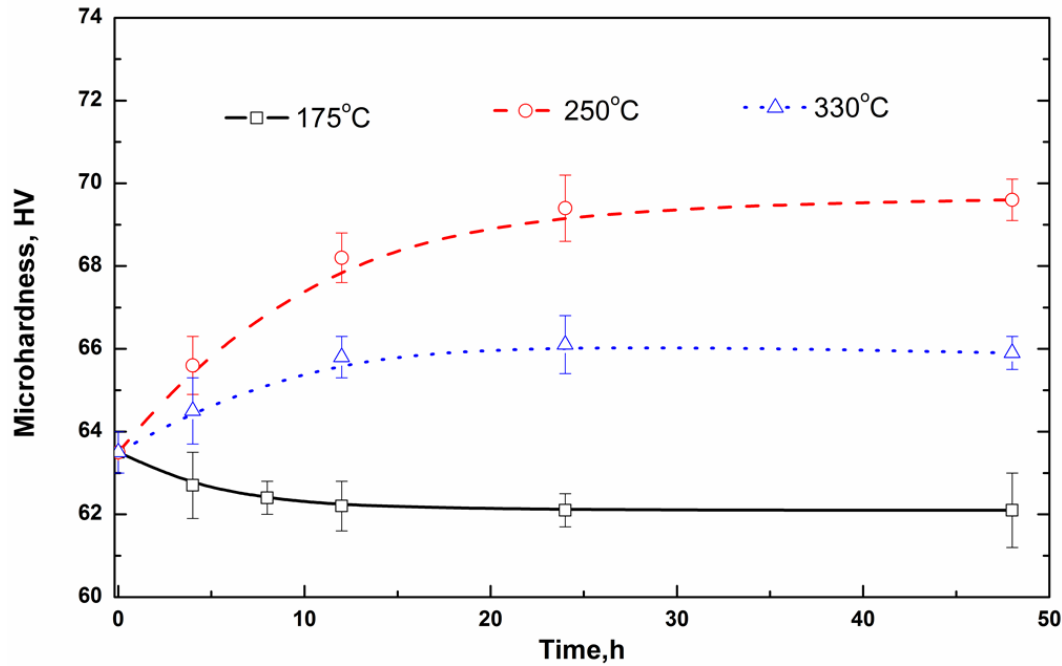
132 **3.1 Influence of the two-step treatment on elevated-temperature properties**

133 Fig. 1 shows the evolution of microhardness of Alloy A after two-step heat
134 treatments with the first step at various temperatures followed by 375°C/48h. The initial
135 point (0 hour) is the microhardness after the single-step heat treatment (375°C/48h). It
136 can be found that the microhardness decreases slightly with time after the two-step heat
137 treatment with the first-step treated at 175 °C compared to the single-step heat treatment.
138 For instance, the microhardness is decreased from 63.5 to 62 HV after treated
139 175°C/24h+375°C/48h. However, the microhardness remarkably increases when first
140 treated at both 250 °C and 330 °C, and it reaches the peak value after 12 to 24 hours.
141 Furthermore, the microhardness is higher when treated at 250 °C than at 330 °C at a
142 given holding time. As shown in Fig. 1, the value of the microhardness is increased from
143 63.5 HV to 66 HV after 330°C/24h+375°C/48h and further to 70 HV after
144 250°C/24h+375°C/48h.

145 In order to evaluate the influence of the two-step treatment on the elevated-
146 temperature properties, the YS and creep properties at 300 °C were measured after two-
147 step heat treatments with various preheating temperatures after 24 hours and results are
148 shown in Fig. 2. It can be seen that the change of properties after various two-step heat
149 treatments in Fig. 2 is similar with the evolution of microhardness in Fig. 1. As shown in
150 Fig. 2a, the YS at 300 °C is lower after the two-step heat treatment when first treated at
151 175 °C (175°C/24h+375°C/48h), but it is higher than the single-step treatment
152 (375°C/48h) when first treated at 250 °C and 330 °C. For instance, the YS at 300 °C after
153 175°C/24h+375°C/48h is 78.6 MPa, which is lower than that after the single-step heat

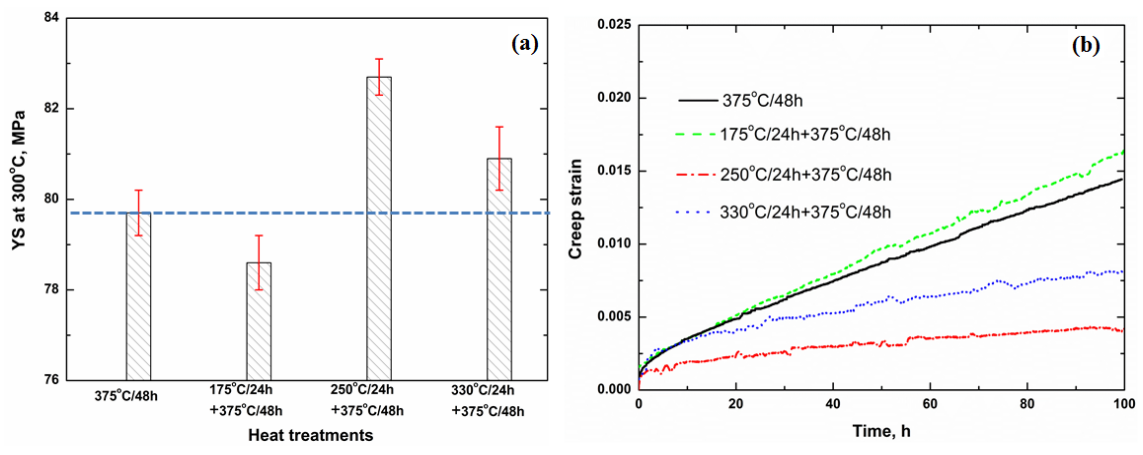
154 treatment (79.7 MPa). However, the YS increases to 81 MP after 300°C/24h+375°C/48.
 155 The highest YS at 300°C is obtained after the two-step heat treatment of
 156 250°C/24h+375°C/48h, which reaches 82.7 MPa.

157
 158
 159
 160
 161
 162
 163
 164
 165
 166
 167



168 Fig. 1 Evolution of microhardness of Alloy A after two-step treatments with the first step
 169 at various temperatures

170
 171
 172
 173
 174
 175
 176



177 Fig. 2 Evolution of elevated-temperature properties of Alloy A after two-step treatments:
 178 (a) YS at 300 °C and (b) typical creep curves at 300 °C

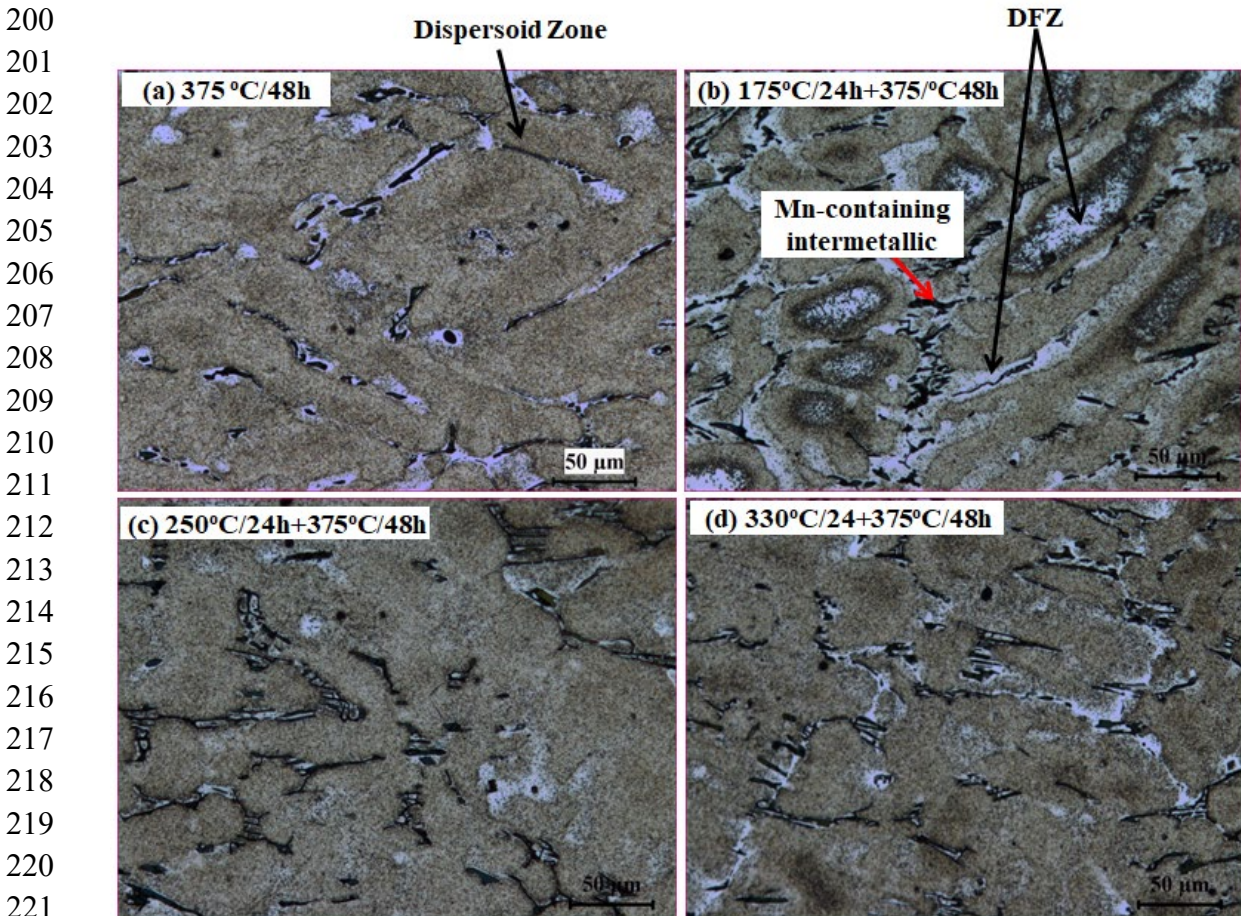
179 Fig. 2b shows the typical creep curves after various two-step heat treatments. It can
 180 be seen that the creep stain after 175°C/24h+375°C/48 is slightly higher than that after
 181 the single-step treatment. However, the creep strain is much low after treated at
 182 330°C/24h+375°C/48 and 250°C/24h+375°C/48. As shown in Fig. 2b, the creep strain
 183 decreases from 0.014 after the single treatment (375°C/48) to 0.008 after

184 330°C/24h+375°C/48 and further to 0.0038 after 250°C/24h+375°C/48. The minimum
185 creep rate is calculated to be $3.9 \times 10^{-8} \text{ s}^{-1}$ after 175°C/24h+375°C/48h, $3.1 \times 10^{-8} \text{ s}^{-1}$ after
186 375°C/48h, $1.6 \times 10^{-9} \text{ s}^{-1}$ after 330°C/24h+375°C/48h and $7.5 \times 10^{-9} \text{ s}^{-1}$ after
187 250°C/24h+375°C/48h, respectively. It is evident that the two-step heat treatment of
188 250°C/24h+375°C/48h possesses the lowest creep strain and the lowest minimum creep
189 rate, indicating the best creep resistance among four heat treatment conditions
190 investigated.

191 3.2 Evolution of dispersoids during two-step heat treatment

192 As shown in Figs. 1 and 2, the microhardness at room temperature as well as the
193 strength and creep resistance at 300 °C can be greatly influenced by the two-step heat
194 treatment. It is apparent that the change of elevated-temperature properties is attributed to
195 the evolution of strengthening phase in the microstructure, namely the precipitation of α -
196 Al(MnFe)Si dispersoids in 3004 alloy during the two-step heat treatment according to the
197 Orowan strengthening mechanism [4, 11, 21].

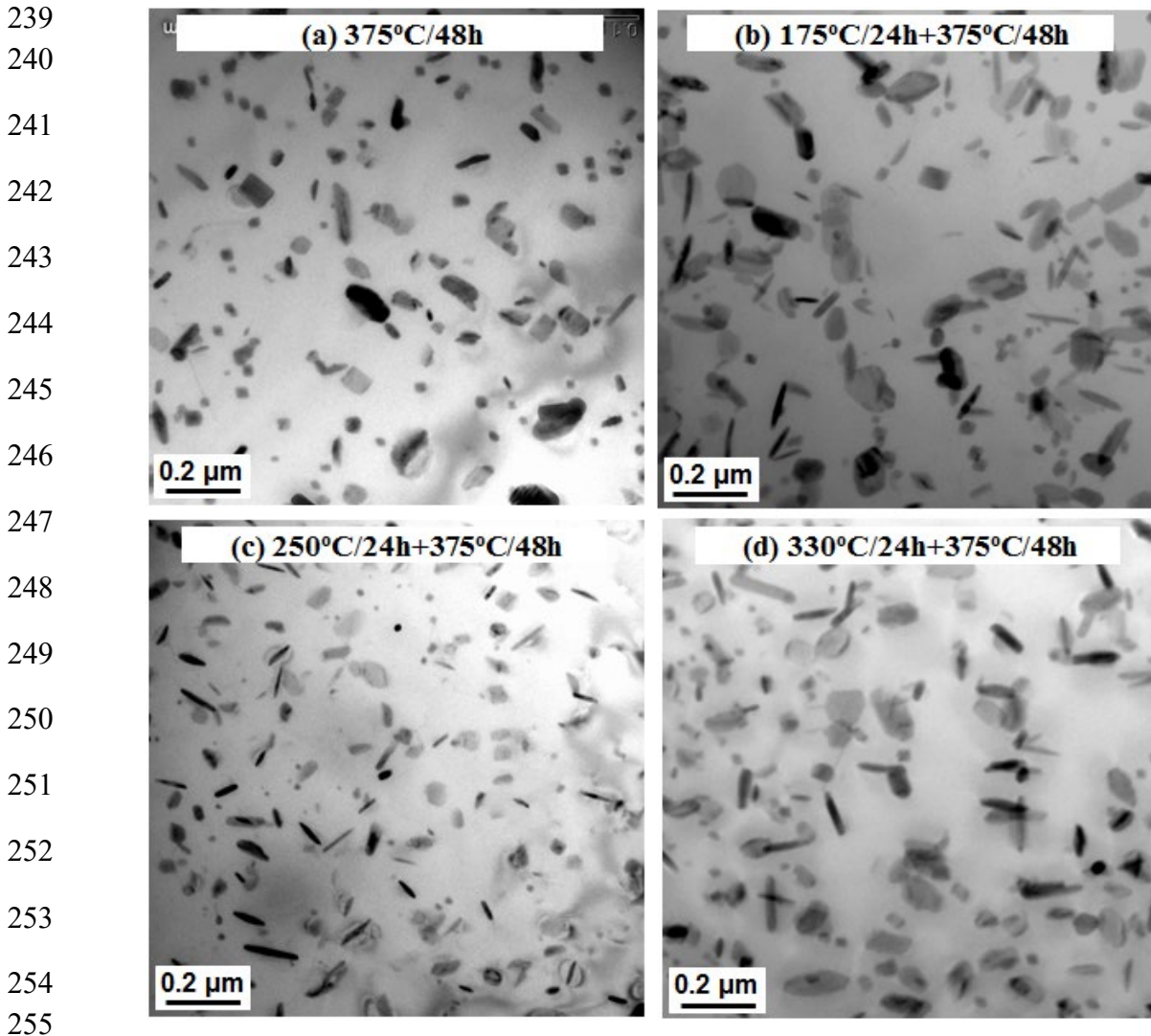
198 The general distribution of dispersoids was first checked in the optical microscopy
199 and results are shown in Fig. 3.



222 Fig. 3 Microstructure of Alloy A after various two-step heat treatments: (a) 375°C/48h;
223 (b) 175°C/24h+375°C/48h; (c): 250°C/24h+375°C/48h and (d): 330°C/24h+375°C/48h

224 It can be found that when pretreated at 250 °C (Fig. 3c) and 330 °C (Fig. 3d), there
225 is no obvious change on the distribution of dispersoids with a minor change on the
226 dispersoids free zone (DFZ) compared to the single-step treatment (Fig. 3a). As shown in
227 Fig. 3a, 3c and 3d, the dispersoids are uniformly distributed in the dendrite cells with the
228 interdendritic DFZ surrounding the intermetallics (the black Mn-containing intermetallics,
229 see the arrow marked in Fig. 3b). In addition, it seems that DFZ is the least in Fig. 3c
230 after pretreated at 250 °C. However, when pretreated at 175 °C (Fig. 3b), the volume of
231 DFZ seems to be higher than other three conditions but the dispersoids are still uniformly
232 distributed in the center of dendrites.

233 In addition, the characteristics of dispersoids in the dispersoid zone after various
234 two-step heat treatments were studied using TEM in more details and results are shown in
235 Fig. 4. According to TEM-EDS results and the literature [2, 7], all dispersoids found here
236 are α -Al(MnFe)Si dispersoids. Since the dispersoids have been identified by TEM with
237 the selected area diffraction pattern (SADP) and EDS in our previous works [2, 7], the
238 TEM-EDS results is not shown in the present work.



256 Fig. 4 Distribution of dispersoids after various heat treatments: (a) 375°C/48h;
257 (b) 175°C/24h+375°C/48h; (c): 250°C/24h+375°C/48h and (d): 330°C/24h+375°C/48h

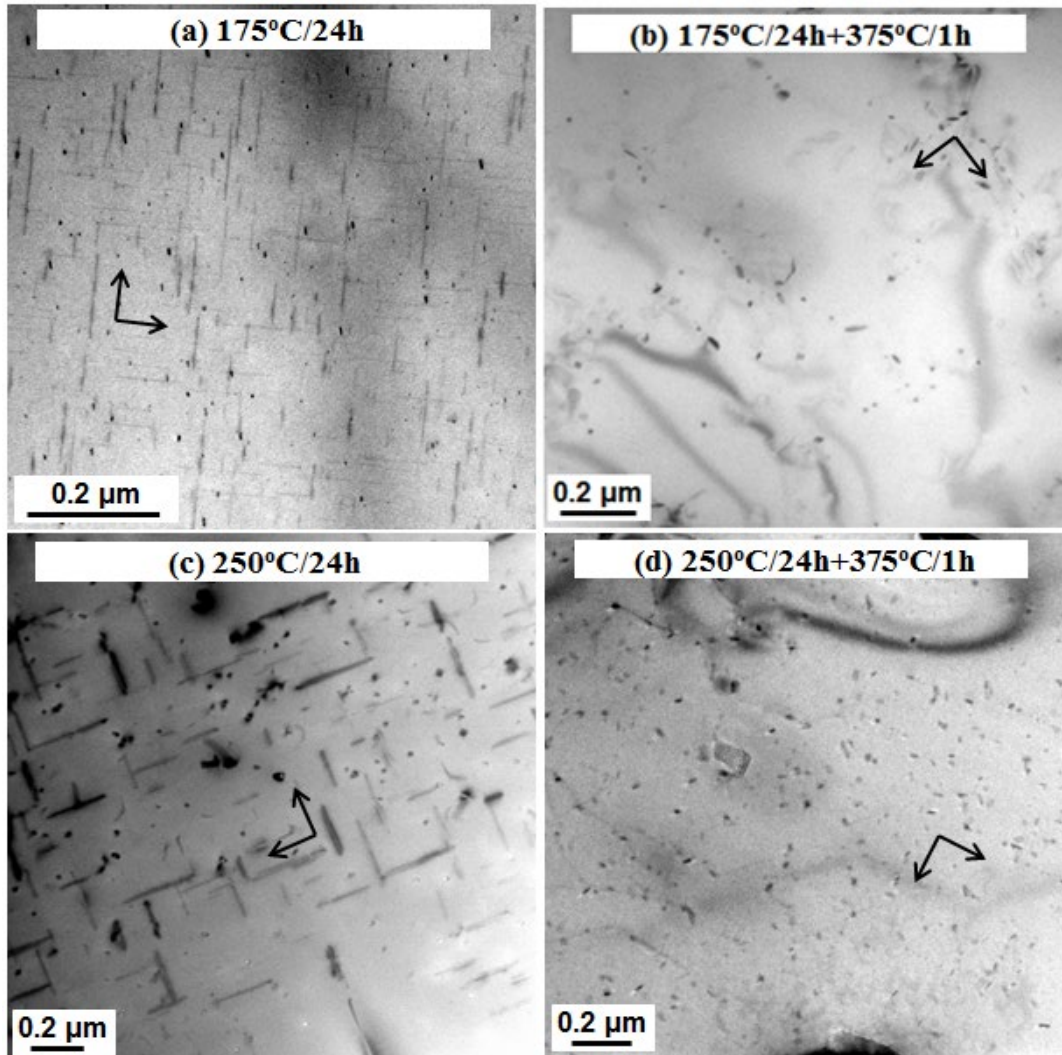
258 Compared to the dispersoids after the single-step heat treatment (375°C/48h) in Fig.
259 4a, the size of dispersoids is larger when pretreated at 175 °C (Fig. 4b). However, when
260 pretreated at 250 °C (Fig. 4c), the size of dispersoids generally becomes smaller. When
261 pretreated at 330 °C, the dispersoids have a similar size (Fig. 4d) with the single-step
262 treatment (Fig. 4a). Therefore, the finer dispersoids (Fig. 4c) combined with less area of
263 DFZ (Fig. 3c) after 250°C/24h +375°C/48h result in the highest strength and creep
264 resistance (Fig. 2) as well as the highest microhardness (Fig. 1). On the other hand, the
265 larger size of dispersoids (Fig. 4b) and more area of DFZ (Fig. 3b) after 175°C/24h
266 +375°C/48h are responsible for the lowest properties.

267 The different characteristics of α -Al(MnFe)Si dispersoids during various two-step
268 heat treatments can be attributed to the formation of pre-existing Mg_2Si in the first-step
269 treatment. The pre-existing Mg_2Si was report to be the nucleation sites of α -Al(MnFe)Si
270 dispersoids [22]. In the present work, it is observed that, during heating process towards
271 375 °C in the single-step treatment, a number of Mg_2Si first precipitated at the
272 temperature range of 150 - 300°C and then slowly dissolved at higher temperatures of
273 300 - 375°C before the beginning of dispersoid precipitation. The temperature range for
274 the precipitation and dissolution of various Mg_2Si is greatly in accordance with the
275 literature [23, 24]. Therefore, two preheating conditions (175°C/24h and 250°C/24h) are
276 selected to study the relationship between the two-step heat treatment and the dispersoid
277 precipitation. Fig. 5a and 5c is the microstructure after the first-step treatments, while Fig.
278 5b and 5d is the initial state of the dispersoid precipitation, which is after 1 hour at
279 375 °C.

280 As shown in Fig. 5a and 5c, a large number of Mg_2Si were precipitated at both
281 conditions (175°C/24h and 250°C/24h). However, there are big differences on the Mg_2Si
282 precipitation, such as the type, size and morphology. When pretreated at 175°C/24h (Fig.
283 5a), only very thin needle-like Mg_2Si can be observed and the average size is measured to
284 be 120(L) x 6(W) nm, which is reported to be the β'' - Mg_2Si [23, 25]. On the other hand,
285 Mg_2Si became coarser with thick lath-shaped and rod-like morphology after 250°C/24h
286 (Fig. 5c). The average size was 430 (L) x 26 (w) nm, which are believed to be β' - Mg_2Si
287 according to the literature [23-27].

288 During the second step of heat treatment, the dispersoids begin to form and the
289 orientation is the same with the pre-existing Mg_2Si (Figs. 5b and d), indicating the
290 nucleation and growth of dispersoids on pre-existing Mg_2Si . However, the number
291 density of dispersoids is remarkably different in two preheating treatments. When
292 pretreated at 175 °C (Fig. 5b), only a small number of dispersoids can be observed.
293 However, it can be clearly seen that when pretreated at 250 °C (Fig. 5d), a large number
294 of dispersoids precipitated and all of them aligned along the original orientation of pre-
295 existing Mg_2Si precipitates. It seems that β' - Mg_2Si with a reasonable size is more

296 appropriate to be the nucleation site of dispersoids than β'' -Mg₂Si. In Figs. 5c and d with
297 preheating at 250°C/24h, β' -Mg₂Si precipitates with thicker lath-shaped and rod-like
298 morphology show the strong promoting effect on the nucleation of dispersoids, leading
299 to the finer dispersoids and the higher volume of dispersoids formed during the following
300 holding process at 375 °C, as shown in Fig. 4c.



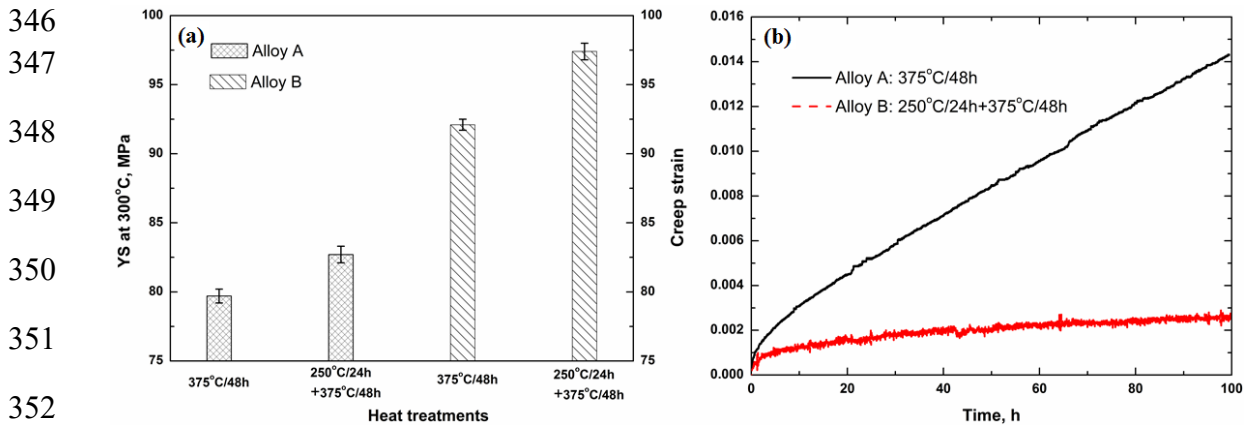
327 Fig. 5 Microstructure of Alloy A at various stages of two-step heat treatments:
328 (a) 175°C/24h; (b) 175°C/24h+375°C/1h; (c): 250°C/24 and (d): 250°C/24h+375°C/1h

329 3.3 Optimization of elevated-temperature properties of Al-Mn-Mg 3004 alloy

330 As discussed in section 3.1, the proper two-step heat treatment, such as
331 250°C/24h+375°C/48h, can remarkably improve the alloy properties. In addition, our
332 previous works [3, 7, 8] have demonstrated that the elevated-temperature properties of
333 Al-Mn-Mg 3004 alloys can be enhanced by adjusting alloying elements. Alloy B in Table
334 1 is designed for an optimized chemical composition by modifying Fe, Mn and Mo [3, 7,
335 8]. Therefore, the two-step heat treatment (250°C/24h+375°C/48h) is applied on Alloy B

336 to explore the attainable alloy properties at elevated temperature for Al-Mn-Mg 3004
337 alloys.

338 The YS at 300 °C of both Alloys A and B after single and two-step heat treatments
339 are shown in Fig. 6a. It can be seen that the YS increases from 80 MPa (Alloy A) to 92
340 MPa (Alloy B) after the single-step heat treatment (375°C/48h) with modified alloying
341 elements. Furthermore, the YS in Alloy B is further improved from 92 MPa after the
342 single-step heat treatment (375°C/48h) to 97 MPa after the two-step heat treatment
343 (250°C/24h+375°C/48h), confirming the synergistic benefit of the two-step heat
344 treatment and modifying alloying elements on enhancing the elevated-temperature
345 properties.



352

353 Fig. 6 Elevated-temperature properties of experimental alloys:

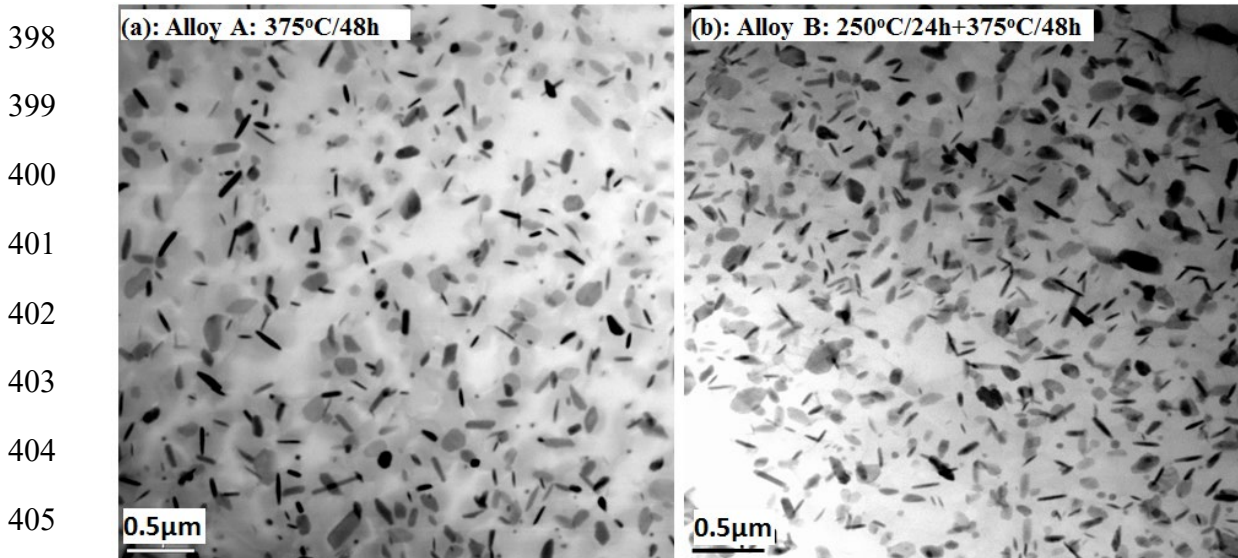
354 (a) YS at 300°C and (b) typical creep curves at 300°C

355 The YS at 300°C of Alloy B after the two-step heat treatment
356 (250°C/24h+375°C/48h) can reach as high as 97 MPa (Fig. 6a), which is 21%
357 improvement on the elevated-temperature strength relative to Alloy A. It is the maximum
358 attainable YS at 300 °C on Al-Mn-Mg 3004 alloys up to now. To explore the
359 improvement of the creep resistance at elevated temperature, the typical creep curves of
360 these two conditions (Alloy B after 250°C/24h+375°C/48h and Alloy A after 375°C/48h)
361 are shown in Fig. 6b. Similar to the YS, the total creep strain has been dropped from
362 0.0142 in Alloy A after 375°C/48h to 0.0025 in Alloy B after 250°C/24h+375°C/48h
363 during creep deformation 100 hours at 300°C. The minimum creep rate decreases from
364 $3.1 \times 10^{-8} \text{ s}^{-1}$ (Alloy A) to $2.2 \times 10^{-9} \text{ s}^{-1}$ (Alloy B), which is one order lower on the minimum
365 creep rate.

366 At the same two-step heat treatment condition (250°C/24h+375°C/48h), the total
367 creep stain and the minimum creep rate of Alloy A are 0.0038 and $7.5 \times 10^{-9} \text{ s}^{-1}$ (Fig. 2b),
368 respectively. Both the total creep strain and the minimum creep rate of Alloy B are lower
369 than that of Alloy A. Taking into account of both data, this is the best creep resistance
370 obtained in Al-Mn-Mg 3004 alloys. These enhanced elevated-temperature properties after
371 modifications of the heat treatment and alloying elements (Alloy B) can be principally
372 attributed to the precipitation of dispersoids (size and volume fraction). Fig. 7 shows that

373 the volume fraction of dispersoids in Alloy B after 250°C/24h+375°C/48h is much higher
374 than Alloy A after 375°C/48h, resulting in the higher elevated-temperature properties in
375 Alloy B after 250°C/24h+375°C/48h.

376 Furthermore, those dispersoids in the aluminum matrix are proved to be thermally
377 stable during the long-time holding at 300-350 °C [2, 7]. Therefore, it is expected to
378 maintain the superior mechanical and creep properties in Alloy B even after
379 long-time exposure at high temperature work condition (300-350 °C). This is one of most
380 significant advantages of dispersoid-strengthening aluminum alloys compared to
381 conventional precipitation-hardening aluminum alloys, such as 2xxx, 6xxx and 7xxx,
382 which exhibit a significant deterioration of mechanical properties during elevated-
383 temperature exposure due to the rapid coarsening of precipitates. For instance, the instant
384 YS at 315°C of AA2024 after peak aging (T6) is 95 MPa, which is at the similar level of
385 the strength as Alloy B in the present work, although AA2024-T6 have the highest YS
386 among the precipitation-hardening wrought aluminum alloy [28]. However, the YS at
387 315°C of AA2024-T6 rapidly dropped to 45 MPa after exposing for 100 hours at 315°C,
388 in which 50% of YS has been lost after thermal holding. The Alloy B can still maintain
389 the similar level of YS as that before the thermal exposing during long-term exposure at
390 350 °C [7]. On the other hand, Al-Mn-Mg 3004 alloys are more economic than other
391 dispersoid-strengthening aluminum alloys with Sc and Zr [29, 30] and much lighter than
392 traditional high temperature alloys, such as Ti and Ni alloys [31, 32]. In the practical
393 view, Al-Mn-Mg 3004 alloys are more competitive in large-scale industrial production,
394 which can be processed with conventional ingot metallurgy route and subsequent
395 thermomechanical processes. Therefore, Al-Mn-Mg 3004 alloys with modified alloying
396 elements and optimized heat treatment are one of the most promising candidates in
397 lightweight aluminum alloys for elevated-temperature applications.



406 Fig. 7 Precipitation of dispersoids in Alloy A and Alloy B under different heat treatments:
407 (a): Alloy A, 375°C/48h and (b): Alloy B, 250°C/24h+375°C/48h

408 4. Conclusions

409 In the present work, the influence of the two-step heat treatment on elevated-
410 temperature properties has been investigated in Al-Mn-Mg 3004 alloys with the
411 following conclusions:

412 (1) When the first preheating temperature is lower (~ 175 °C), the alloy properties
413 decrease gradually with prolonging holding time, while they increase remarkably when
414 first treated at higher temperature (250-330 °C) during two-step heat treatments. The
415 maximum elevated-temperature strength and creep resistance are obtained after the two-
416 step heat treatment of 250°C/24h+375°C/48h with finer dispersoids and higher volume
417 fraction of dispersoids.

418 (2) The formation of dispersoids is greatly related to the type and size of pre-existing
419 Mg₂Si precipitated during the first-step treatments, in which coarse rod-like β' -Mg₂Si
420 strongly promotes the nucleation of dispersoids while the fine needle-like β'' -Mg₂Si
421 shows less influence.

422 (3) Under optimized two-step heat treatment (250°C/24h+375°C/48h) and modified
423 alloying elements (Fe, Mn and Mo), the yield strength at 300 °C of Al-Mn-Mg 3004
424 alloys can reach as high as 97 MPa with the minimum creep rate of 2.2×10^{-9} s⁻¹ at 300 °C,
425 enabling them as one of the most promising candidates in lightweight aluminum alloys
426 for elevated-temperature applications.

427 Acknowledgments

428 The authors would like to acknowledge the financial support of the Natural Sciences
429 and Engineering Research Council of Canada (NSERC) and Rio Tinto Aluminum
430 through the NSERC Industry Research Chair in the Metallurgy of Aluminum
431 Transformation at University of Quebec at Chicoutimi.

432 References

- 433 [1] Y. J. Li, A. M. F. Muggerud, A. Olsen and T. Furu: *Acta Mater.*, 2012, vol. 60, pp.
434 1004-14.
435 [2] K. Liu and X. G. Chen: *Mater. Des.*, 2015, vol. 84, pp. 340-50.
436 [3] K. Liu and X. G. Chen: *Metall. Mater. Trans. B*, 2015, vol. 47B, pp. 3291-300.
437 [4] Y. J. Li and L. Arnberg: *Acta Mater.*, 2003, vol. 51, pp. 3415-28.
438 [5] R. Kamat: *JOM*, 1996, vol. 48, pp. 34-38.
439 [6] Q. Du, W. J. Poole, M. A. Wells and N. C. Parson: *Acta Mater.*, 2013, vol. 61, pp.
440 4961-73.
441 [7] K. Liu, H. Ma and X. G. Chen: *J. Alloys Compd.*, 2017, vol. 694, pp. 354-65.
442 [8] K. Liu and X.-G. Chen: *J. Mater. Res.*, 2017, vol. 32, pp. 2585-93.
443 [9] K. Liu, A. M. Nabawy and X.-G. Chen: *Trans. Nonferrous Met. Soc. China*, 2017, vol.
444 27, pp. 771-78.
445 [10] H.-W. Huang and B.-L. Ou: *Mater. Des.*, 2009, vol. 30, pp. 2685-92.

- 446 [11] A. M. F. Muggerud, E. A. Mørtzell, Y. Li and R. Holmestad: *Mater. Sci. Eng., A*,
447 2013, vol. 567, pp. 21-28.
- 448 [12] Y. Li and L. Arnberg: *Essential Readings in Light Metals* John Wiley & Sons, Inc.,
449 Hoboken, NJ, USA, 2013, vol. 3, pp. 1021-27.
- 450 [13] K. Liu and X. G. Chen: *Materials Science and Engineering A*, 2017, vol. 697, pp.
451 141-48.
- 452 [14] Y.-L. Deng, Y.-Y. Zhang, L. Wan, A. Zhu and X.-M. Zhang: *Metall. Mater. Trans.*
453 *A*, 2013, vol. 44, pp. 2470-77.
- 454 [15] Z. Guo, G. Zhao and X. G. Chen: *Mater. Charact.*, 2015, vol. 102, pp. 122-30.
- 455 [16] Z. Jia, G. Hu, B. Forbord and J. K. Solberg: *Materials Science and Engineering A*,
456 2008, vol. 483-484, pp. 195-98.
- 457 [17] X.-y. LÜ, E.-j. Guo, P. Rometsch and L.-j. Wang: *Trans. Nonferrous Met. Soc.*
458 *China*, 2012, vol. 22, pp. 2645-51.
- 459 [18] J. D. Robson: *Materials Science and Engineering A*, 2002, vol. 338, pp. 219-29.
- 460 [19] P. X. Liu, Y. Liu and R. Xu: *Trans. Nonferrous Met. Soc. China*, 2014, vol. 24, pp.
461 2443-51.
- 462 [20] E. R. Weibel and H. Elias: *Quantitative methods in morphology*, Springer-Verlag,
463 Berlin; New York, 1967.
- 464 [21] A. R. Farkoosh, X. Grant Chen and M. Pekguleryuz: *Mater. Sci. Eng., A*, 2015, vol.
465 620, pp. 181-89.
- 466 [22] L. Lodgaard and N. Ryum: *Mater. Sci. Eng., A*, 2000, vol. 283, pp. 144-52.
- 467 [23] J. Osten, B. Milkereit, C. Schick and O. Kessler: *Materials*, 2015, vol. 8, pp. 2830-
468 48.
- 469 [24] Y. Ohmori, L. Doan, nbsp, Chau and K. Nakai: *Mater. Trans.*, 2002, vol. 43, pp.
470 246-55.
- 471 [25] A. Gaber, M. A. Gaffar, M. S. Mostafa and A. F. Abo Zeid: *Mater. Sci. Technol.*,
472 2006, vol. 22, pp. 1483-88.
- 473 [26] L. Doan, nbsp, Chau, K. Nakai, Y. Matsuura, S. Kobayashi, et al.: *Mater. Trans.*,
474 2002, vol. 43, pp. 1371-80.
- 475 [27] Y. Birol: *Trans. Nonferrous Met. Soc. China*, 2013, vol. 23, pp. 1875-81.
- 476 [28] J. G. Kaufman: *Properties of aluminum alloys : tensile, creep, and fatigue data at*
477 *high and low temperatures*, ASM International ; Aluminum Association, Materials Park,
478 Ohio; Washington, D.C., 1999.
- 479 [29] C. Booth-Morrison, D. C. Dunand and D. N. Seidman: *Acta Mater.*, 2011, vol. 59,
480 pp. 7029-42.
- 481 [30] K. E. Knipling, D. C. Dunand and D. N. Seidman: *Acta Mater.*, 2008, vol. 56, pp.
482 114-27.
- 483 [31] X. M. Chen, Y. C. Lin, M. S. Chen, H. B. Li, D. X. Wen, J. L. Zhang, et al.: *Mater.*
484 *Des.*, 2015, vol. 77, pp. 41-49.
- 485 [32] T. Wang, C. Wang, W. Sun, X. Qin, J. Guo and L. Zhou: *Mater. Des.*, 2014, vol. 62,
486 pp. 225-32.

487

488

489

490

491 Table 1 Chemical composition of experimental alloys in present work

Alloy	Elements (wt. %)					
	Mn	Mg	Si	Fe	Mo	Al
A (base)	1.26	1.08	0.24	0.56	0	Bal.
B	1.52	1.11	0.26	0.29	0.28	Bal.

492

493 **Figure Captions:**

494 Fig. 1 Evolution of microhardness of Alloy A after two-step treatments with the first step
495 at various temperatures

496

497 Fig. 2 Evolution of elevated-temperature properties of Alloy A after two-step treatments:
498 (a) YS at 300 °C and (b) typical creep curves at 300 °C

499

500 Fig. 3 Microstructure of Alloy A after various two-step heat treatments: (a) 375°C/48h;
501 (b) 175°C/24h+375°C/48h; (c): 250°C/24h+375°C/48h and (d): 330°C/24h+375°C/48h

502

503 Fig. 4 Distribution of dispersoids after various heat treatments: (a) 375°C/48h;
504 (b) 175°C/24h+375°C/48h; (c): 250°C/24h+375°C/48h and (d): 330°C/24h+375°C/48h

505

506 Fig. 5 Microstructure of Alloy A at various stages of two-step heat treatments:
507 (a) 175°C/24h; (b) 175°C/24h+375°C/1h; (c): 250°C/24h and (d): 250°C/24h+375°C/1h

508

509 Fig. 6 Elevated-temperature properties of experimental alloys:
510 (a) YS at 300°C and (b) typical creep curves at 300°C

511

512 Fig. 7 Precipitation of dispersoids in Alloy A and Alloy B under different heat treatments:
513 (a): Alloy A, 375°C/48h and (b): Alloy B, 250°C/24h+375°C/48h